Common-Mode Cancellation in Sinusoidal Gating With Balanced InGaAs/InP Single Photon Avalanche Diodes

Joe C. Campbell, *Fellow, IEEE*, Wenlu Sun, Zhiwen Lu, Mark A. Itzler, and Xudong Jiang

***Abstract*— We demonstrate a sinusoidal-gated InGaAs/InP single photon avalanche diode (SPAD) pair with high photon detection efficiency (PDE) and low dark count rate (DCR). The photodiode pair is biased in a balanced configuration with only one of the SPADs illuminated. The advantage of balanced detectors is cancellation of the common component of the output signal, which in this case arises from sinusoidal gating. In conventional sinusoidal gating, narrow-band RF filters are used to eliminate the gating signal while imparting minimal change to the avalanche pulses. A disadvantage of this approach is that the requisite filters fix the operating frequency, whereas the balanced SPAD receiver is frequency agile. At a laser repletion rate of 1 MHz and a temperature of 240 K, the DCR and PDE are 58 kHz and 43%, respectively. The afterpulse probability is lower than a single sinusoidal-gated SPAD. Jitter of 240 ps is achieved with one photon per pulse and an excess bias of 1.6%.**

***Index Terms*— Avalanche breakdown, avalanche photodiodes, infrared detectors, jitter, noise cancellation, optical receivers, optoelectronic and photonic sensors, RF signals, signal to noise ratio.**

I. Introduction

SINGLE photon receivers are widely used in applications such as high-resolution spectroscopy, fluorescence measurement, astronomy, and quantum information technology (quantum computing and quantum key distribution). Among the candidates for single photon detection, InGaAs/InP SPADs have been widely studied for communications applications, e.g., fiber optic quantum key distribution [1]–[5]. To determine the quantum states or discriminate the quantum bits, SPADs are usually operated in a synchronized Geiger mode. The most widely used approach is gated mode operation, which has the attributes of high photon detection efficiency (PDE) and low dark count rate (DCR). However, in gated mode, the transient signal at the leading and trailing edges of the excess bias pulses can obscure the faint avalanche signals triggered by single photons. To cancel the transient spikes, various methods have been proposed and demonstrated. Bethune and Risk [6] have utilized two matched delay lines to cancel the transient spikes. Tosi et al. [7] have demonstrated a "dummy path" approach, where a matched capacitor reproduces the spurious peaks, which are compared with the output signal of the SPAD using a high speed comparator. By this means the transient spikes of SPADs are suppressed. Another transient cancellation technique, self differencing, has enabled operation and data transmission up to 315 MHz [8]. In self differencing, the SPAD output signal is split and one arm is inverted and delayed by one clock period. When the signals are recombined, the transient signals cancel. Self-differencing can also be achieved with balanced detectors [9]. Tomita and Nakamura have used dual SPADs biased in parallel with differential detection [10]. A 180° hybrid was employed at the output to produce out-of-phase signals for differential detection. Another gating approach is sinusoidal gating [3], [4], [11], [12]. For sine wave gating the capacitive response of the sinusoidal bias is a sinusoidal output signal at the same frequency; therefore, it can be removed by a narrow-band notch filter at the output without affecting the spectrally broad avalanche signal. A hybrid combination of self differencing and sine wave gating has also been reported [2].

The ultimate goal with SPADs is to achieve low DCR and high PDE. For III-V compound SPADs a dominate contributor to dark counts, especially at high repetition rate, is afterpulsing. Afterpulsing refers to avalanche events that originate from the emission of carriers that were trapped on deep level traps in the multiplication region during previous avalanche events. The emitted carriers are indistinguishable from those created by the absorption of photons and, thus, have the same avalanche breakdown probability. The lifetimes of the trapped carriers in the InGaAs/InP material system can be as long as 100 μs [13], [14], which greatly restricts the repetitive bias rate and thus the data rate. The most straightforward approach to eliminate afterpulsing is to reduce the photon transmission rate to $\sim$100 kHz in order to permit all trapped charges to be emitted. However, such low data rates are too restrictive for many applications. It has been found that reducing the total charge flow is the most practical solution for suppressing afterpulsing. Using various quenching techniques, this is accomplished by utilizing very short excess bias signals with rapid quenching [3]–[9]. A very effective method to reduce the charge flow in an avalanche event, which has proved effective in reducing afterpulsing, is passive quenching with active reset (PQAR) [13], [15], [16]. This quenching and recharge circuit uses the high impedance of an FET in its "off"

Manuscript received July 28, 2012; revised September 11, 2012; accepted September 26, 2012. Date of publication October 10, 2012; date of current version October 23, 2012.

J. C. Campbell, W. Sun, and Z. Lu are with the Electrical and Computer Engineering Department, University of Virginia, Charlottesville, VA 22904 USA (e-mail: jcc7s@virginia.edu; ws8zp@virginia.edu; zl2a@virginia.edu).

M. A. Itzler and X. Jiang are with Princeton Lightwave Inc., Cranbury, NJ 08512 USA (e-mail: mitzler@princetonlightwave.com; xjiang@princetonlightwave.com).

Color versions of one or more of the figures in this paper are available online at http://ieeexplore.ieee.org.

Digital Object Identifier 10.1109/JQE.2012.2223200

0018–9197/$31.00 © 2012 IEEE

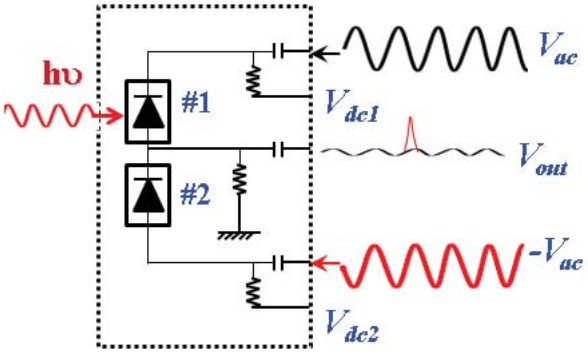

Fig. 1. Balanced receiver layout.

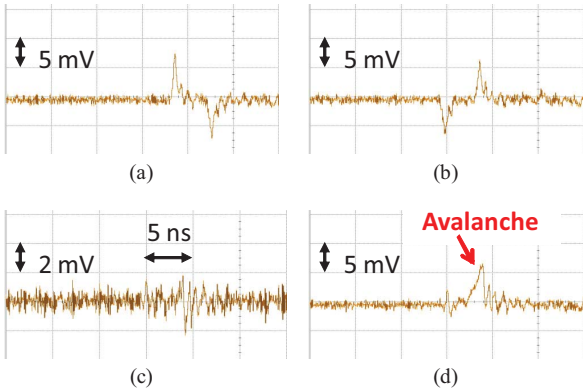

Fig. 2. (a) and (b) Oscilloscope traces for bias pulses applied individually to either diode 1 or diode 2. (c) Cancellation when both diodes are biased simultaneously. (d) Trace for an avalanche event in one diode.

state to provide fast passive quenching. After a specified delay the FET is switched "on" to enable rapid rearming to detect subsequent photons. Further efforts developed this technique for gated mode operation with reduced excess bias duration. In the gated-PQAR operation and at 230 K, afterpulsing probability of 0.5% was achieved with 30% PDE at 100 ns hold off time and 1 MHz repetition rate [14].

Advantages of sinusoidal gating are facile generation of short excess bias pulses and excellent signal to noise performance. While sinusoidal gating has achieved high PDE and low DCR, one of its limiting factors for some applications is that the operation frequency is fixed owing to the narrow band filters that are required to remove the gating signal from the SPAD output. In this paper we use the balanced detector configuration that has been widely employed for coherent detection in optical communications to cancel common-mode signals such as laser relative intensity noise (RIN). This approach eliminates the RF filters permitting data transmission at any sub harmonic of the gate frequency. A balanced detector pair is usually applied to detect the small signal difference between the two channels. The two photodiodes are both reverse biased and connected to opposite AC voltage swings. They compete to affect the voltage at the common node (V_{out} in Figure 1) by producing a small difference in the current flow. The configuration of balanced detectors enables the cancellation of common mode signals between the two detectors. Compared with a conventional single detector, it has been shown that balanced detectors can improve system sensitivity by 15–20 dB [17]. We have utilized this detector configuration to detect the small avalanche current generated by single photons in one diode of the balanced SPAD pair. This approach is similar to differential detection [18] except that it does not require additional components in the output circuitry [10]. We demonstrate high PDE, low DCR, and reduced afterpulsing.

II. Experimental Setup

A modified conventional sinusoidal counting system described in [5] has been adopted for this work. Avalanche events were registered with a PicoHarp 300 multi-channel analyzer, which has a maximum synchronization rate of 80 MHz. Thus all the experiments were performed at or below this gating rate. The counter has an 80 ns dead time, which is the time that the counter requires to reset its electronics after registering a count. To operate the sinusoidal system for balanced APDs, the sinusoidal gated system in [5] was modified to provide two opposite phase sinusoidal input signals (Figure 1).

III. Performance and Analysis

The cancellation characteristics of the photodiode pair are illustrated in Fig. 2 for the case of pulse gated operation. The two upper oscilloscope traces, Fig. 2(a)–(b), show the diode pair output with 5 ns bias pulses applied to each diode. Cancellation is illustrated in Fig. 2(c) where both diodes are pulse biased simultaneously. (Note that the vertical scale for this trace is 2 mV/div, while that for the others is 5 mV/div.) It is clear that the leading and trailing edge transients have been cancelled. Finally, Fig. 2(d) shows the output for an avalanche event in diode #1. The avalanche signal can easily be distinguished and counted with low error rate. The amplitude is approximately one tenth that observed for conventional pulsed gating, which portends reduced afterpulsing. The degree of transient signal cancellation depends on many factors, such as the dark current of the diode pair, asymmetric parasitics, alignment of the two AC bias pulses, perturbations caused by avalanche events, and mismatch in the transmission lines. It is essential that the input bias signals are 180° out of phase and that they have the same amplitude. In this work this has been accomplished with an attenuator and a phase compensator in one of the input paths. It is also important to ensure the symmetry of the photodiode pair and the circuit layout. Figure 3 shows measured capacitance of two packaged diodes before they were mounted to the circuit board; the difference is <1 fF. In this work the receiver circuit in Fig. 1 was fabricated by hybrid integration. Greater symmetry and better common mode cancellation is anticipated with monolithic integration.

Initial sine wave gating measurements were made with a multi-channel analyzer. The gating rate was 80 MHz and the laser repetition rate was in the range 400 kHz to 10 MHz (dividing the driving sine wave signal by 200 to 8). Figure 4 shows the counts histogram from which the photon counts, dark counts and afterpulses, can be extracted. After setting an appropriate threshold and aligning the laser pulse with a peak of the sine wave gate on the illuminated SPAD, a counts histogram was collected using the multi channel analyzer. The threshold was adjusted to be close but above the noise floor. Figure 4 shows the counts in 14 ns windows; the small peaks

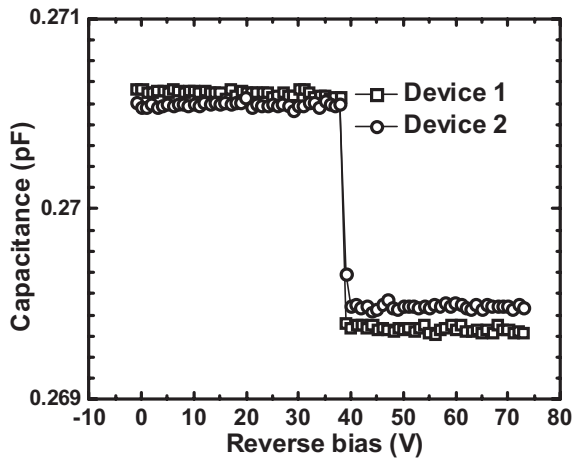

Fig. 3. Capacitance of the diodes twin at reverse bias.

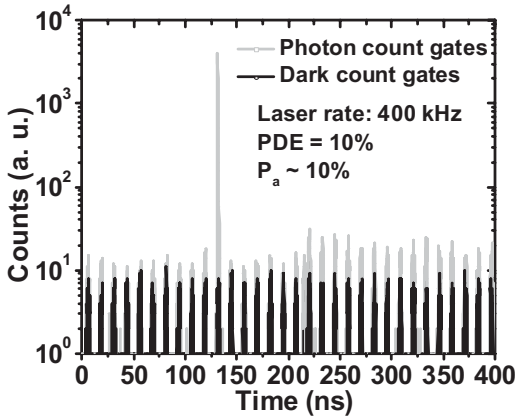

Fig. 4. Counts histogram collected with integration mode of the multichannel analyzer. The highest peak stands for the gate coinciding with the laser pulse; other small peaks are the dark counts from each gate.

are the dark counts, while the largest peak at the 130 ns point in the figure shows the photon counts. Since the repetition rate of laser pulses was 400 kHz, the photon count peaks were separated by 2.5 μs, which explains why only one photon window is shown. In [3], [4], [19], it has been reported that the histogram can be used to calculate afterpulse probability using the relation

$$P_a = \frac{(C_{NI} - C_D)R}{(C_I - C_{NI})} \tag{1}$$

where C_I and C_{NI} represent the average count per gate for the illuminated and non-illuminated gates, respectively (photon count gates in Figure 4). C_D is the dark count per gate with no light incidence for all gates (dark count gates in Figure 4). R is the ratio between the gating rate and the laser rate; in the case of Fig. 4 the value is 200. The excess bias was set to achieve 10% PDE; in this case, the photon count rate is 4×10^3 s^{-1}. The estimated total afterpulse probability is approximately 10%. Note that the dark counts increase due to afterpulsing in the channels after the 210 ns point, which is 80 ns after the photon window at 130 ns. This is due to the 80 ns dead time of the counter.

The balanced SPADs were also characterized using the Time-Tagged-Time-Resolved (TTTR) mode of the multi

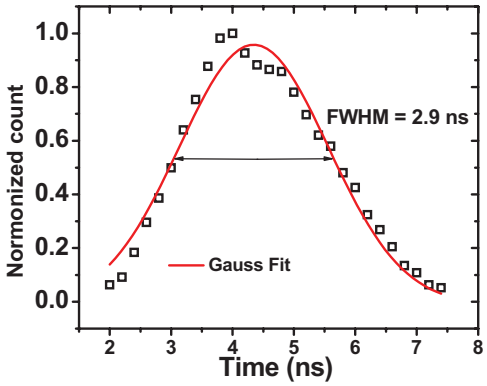

Fig. 5. Effective pulse width of 70 MHz gating rate with laser pulse width of 40 ps for balanced diodes at 200 K.

channel analyzer. This mode (T3) uses one channel for the synchronization signal and the other channel as a counter. The timing resolution of this mode can be as low as 4 ps with the register information of each count. The sine wave gating rate was changed to 70 MHz and the laser repetition rate was in the rage of 350 kHz to 10 MHz. The laser pulse width was 40 ps at wavelength of 1310 nm. The technique to determine PDE and DCR (equations (2) and (3)) that was used in Ref [20] for conventional pulsed gating, was modified to apply to sine wave gating using the following expressions

$$DCR \times \tau_e = -\ln(1 - P_d) \tag{2}$$

$$\text{PDE} = \frac{1}{n} \ln\left(\frac{1 - P_d}{1 - P_t}\right). \tag{3}$$

The effective pulse width, τ_e, was determined by tuning the delay time of the laser pulse and measuring the full width at half maximum of the temporal distribution of the photon counts, which is plotted in Fig. 5. Assuming a Gaussian distribution the full width at half maximum (FWHM) was 2.9 ns.

Figure 6(a) shows the DCR versus PDE for a single SPAD and the balanced SPAD pair for different gating frequencies. For both single and dual SPAD receivers, the DCR versus PDE slope increases with the laser repetition rate. Possible explanations are (1) higher laser repetition rate results in higher afterpulse probability and/or (2) incomplete recharge after frequent avalanche events [5]. It was found that for laser repetition rate $\geq$10 MHz, the PDE is restricted to $<$30% due to the fast rising dark count probability [2]–[4], [11], [12]. The best result with balanced SPADs is 43% PDE and 58 kHz DCR with 1 MHz laser repetition rate. At photon detection efficiency of $\sim$10%, the DCR is 9.6 kHz and the equivalent dark count probability is 2.8×10^{-5}. In Fig. 6(b) we also compare the balanced SPADs with gated quenching and gated-PQAR. At 1 MHz repetition rate, the DCR of the dual SPADs is slightly lower than that of gated quenching at 100 kHz with the same PDE.

Afterpulsing for the dual SPADs was also characterized using the coincidence window method [2], [12]. For these measurements a Stanford Research SR400 counter was used in gated mode. The temporal position of the counter gate was scanned over several periods of the sine wave gates. The counter gate width was set to be 50 ns. This provided

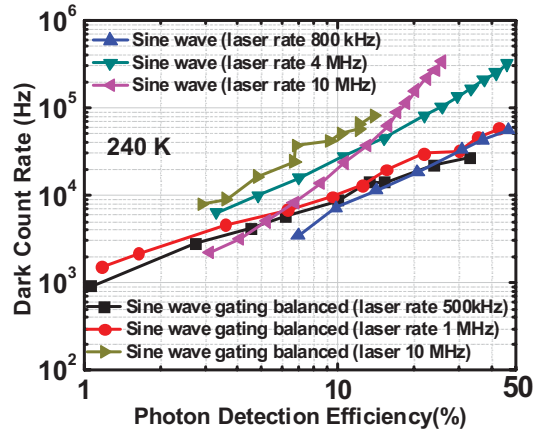

(a)

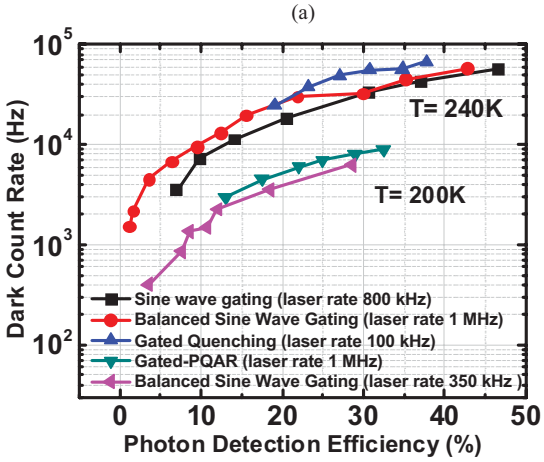

(b)

Fig. 6. (a) DCR versus PDE results from single and dual SPADs with different laser repetition rates. (b) DCR and PDE comparison with other gating schemes.

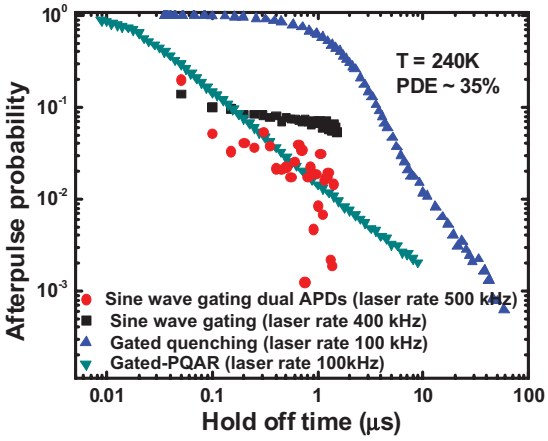

Fig. 7. Afterpulse probabilities of single and dual SPADs with different gating schemes and laser repetition rates, and similar PDE.

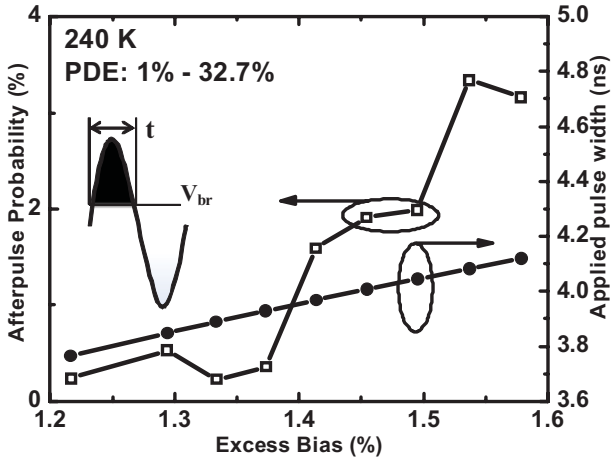

Fig. 8. Afterpulse probabilities at 1-μs holdoff time versus peak excess bias. Right axis shows the applied pulse width.

a temporal distribution of counts similar to Fig. 4 except with more precise count rate information. The afterpulse probability was calculated from the ratio of the afterpulse counts to the photon counts. A relevant phenomenon is the dark count cancellation effect. Figure 7 shows that the afterpulse probability of dual SPADs is smaller than that of single SPADs. Also the dual SPAD curve is not as flat as that for sine wave gating of a single SPAD. We attribute this to the cancelling effect between the two SPADs. This is similar to the transient cancellation shown in Figure 3. If the two SPADs register dark counts at the same time, the resulting avalanche pulses will cancel, which results in a decreased number of dark counts. This is more significant for high dark count rates, especially when afterpulsing is high. Therefore the afterpulse probabilities within 1 μs hold off time exhibit a random pattern as a result of the cancellation effect. The afterpulse probability of the dual SPADs for 1 μs hold off time is only 1% with PDE of 35%; owing to the scatter in the data, the afterpulse probabilities at 0.95, 1 and 1.05 μs hold off times were averaged. Overall, the afterpulse probability for sine wave gating of the dual SPADs at 500 kHz is comparable to that for gated PQAR at 100 kHz.

It has been reported that the afterpulsing decreases faster than linearly with decreasing applied pulse width [21] where we define the applied pulse width as the time period when the diode is biased above breakdown voltage. An advantage of sinusoidal gating at high frequencies is that it is straightforward to achieve very narrow excess bias pulses, which restricts charge flow and reduces afterpulsing. On the other hand, afterpulsing decreases with lower excess biases. Consequently, a useful parameter is the integrated excess bias over the applied pulse width, which we will designate as Δ. For gated quenching, the applied pulse width is a constant that does not depend on excess bias [21], which is not the case for sinusoidal gating, as illustrated in Fig. 8. For sine wave gating, the excess bias can be increased by increasing the DC bias with fixed AC voltage swing or increasing the AC voltage swing for fixed DC bias. Figure 8 shows the measured afterpulse probability and the applied pulse width versus various peak excess biases.

Figure 9 compares computed values of Δ for the different gating schemes in Fig. 7. For the four gating schemes, Δ (y axis) for gated quenching is the highest, which explains the highest afterpulse probability in Fig. 7. The comparable value of Δ for the three other gating methods is consistent with the similar afterpulse probabilities shown by the three overlapping trends in Fig. 7. This indicates that Δ is closely linked to the afterpulsing probability.

Δ is also an indicator for photon detection efficiency as shown in Fig. 10. Both photon detection efficiency and

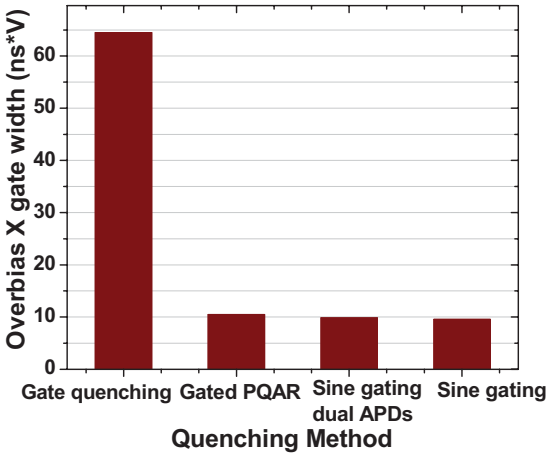

Fig. 9. Comparison of different gating schemes in respect to the integrated gate width with over bias for data in Fig. 7.

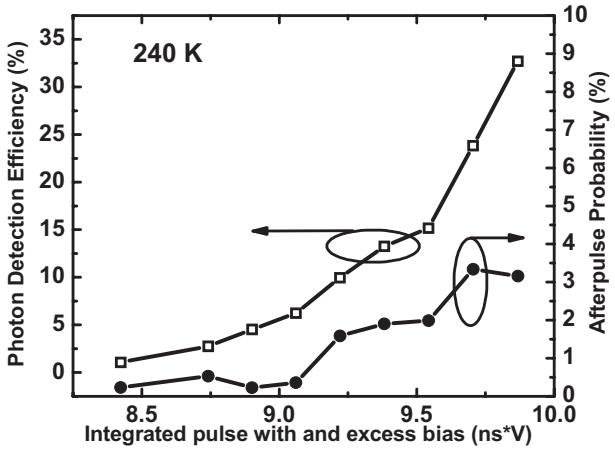

Fig. 10. Indicator for afterpulse probability-integrated pulse width with excess bias. Afterpulse probability is the value at holdoff time of 1 μs.

afterpulse probability increase with Δ; the increase becomes more abrupt as Δ exceeds 9 ns* V. Unfortunately it is not trivial to suppress afterpulsing and simultaneously maintain high PDE by adjusting Δ. For sine wave gating Fig. 8 shows that the applied pulse width increases with increasing peak excess bias. The higher the sine wave gating rate the narrower are the applied excess bias pulses, which would lead to reduced afterpulsing. However, this is somewhat over simplified because higher gating rates also mean there are more excess bias gates within a given time period. The total time that the SPAD is biased above breakdown must be considered. To elucidate this frequency dependence, Δ has been calculated with the total excess duration in a certain time period (the shaded area shown in Figure 11) for different gating frequencies using the following relations

$$\Delta_1 = \int_{\frac{T}{2\pi}\arcsin\alpha}^{\frac{T}{2\pi}(\pi-\arcsin\alpha)} A\sin(\omega t)dt = \frac{2A}{\omega}\sqrt{1-\alpha^2} \quad (4)$$

$$\Delta_2 = Area \times f = \frac{A}{\pi}\sqrt{1-\alpha^2} \quad (5)$$

Equation (4) yields the integrated area for one period (Δ_1) and equation (5) is the total value in one second (Δ_2).

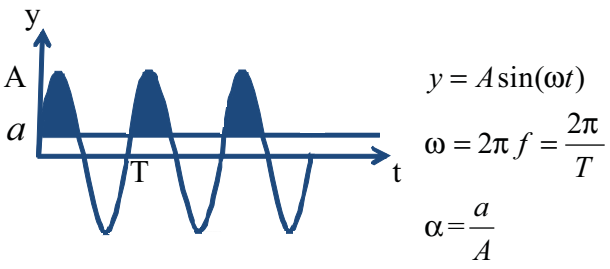

Fig. 11. Sketch and equations illustrating calculation for overall time when the device is biased beyond breakdown. T is the period of sinusoidal wave, A is the peak value of the sine wave, a is the breakdown voltage, and ω is the sine wave frequency.

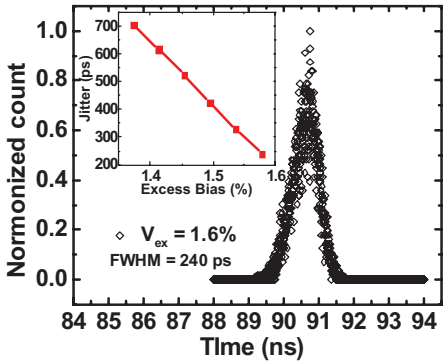

Fig. 12. Temporal distribution of photon counts with different excess bias at 240 K. Inset: jitter of dual SPADs setup.

Equation (5) shows that the value of Δ_2 is actually independent of the gating rate. In other words, for the same peak excess bias, the total time that the device is biased above breakdown is independent of the gating frequency. If we only consider this averaging effect, lower gating frequency yields higher photon detection efficiency and comparable afterpulse probability. Equation (5) also shows that the primary factor that affects the value of Δ is the difference between peak bias and breakdown voltage.

Viewing the frequency independence of Δ in terms of detrapping speed reveals another important aspect of sine wave gating. In Figure 7, the slope of afterpulse probability versus hold off time is smaller for both sinusoidal gating cases than that for gated quenching, i.e., the afterpulse probability decreases at a slower rate with longer hold off time in the case of sinusoidal gating. This is related to the additional bias gates between two adjacent illuminated gates. Among all the photon count windows shown in Figure 4, out of 200 excess bias gates, only one of them is illuminated by a laser pulse. However, a characteristic of sine wave gating is that an excess bias is applied in the other 199 gates.

Recent re-interpretation of afterpulse behavior has provided insight on the detrapping process in InGaAs/InP SPADs, where the detrapping speed can be studied by fitting the afterpulse probability curve versus hold off time with a power law $P_a \propto T^{-\alpha}$; P_a is the afterpulse probability and T is the hold off time [5], [21], [22]. The larger α, the faster detrapping occurs. The reported α for conventional gated-mode operation with various gate widths is $\sim$1 [21], [22], while α obtained from sinusoidal gating for different devices and PDE are all $<$1 [5].

The indicated difference in detrapping speed due to different gating schemes is consistent with the data in Fig. 7.

Jitter measured at different excess bias is shown in the inset of Figure 12. The minimum jitter was 240 ps with 1.6% excess bias (Fig. 12). Measurements of timing jitter not only depend on the device under test but are also related to the characterization condition and the experimental set up, e.g., the spatial and temporal non-uniformity in excess bias [22]. In other words, the excess bias is not distributed evenly across the device and the amplitude of pulses in the pulse train also fluctuates with time. Therefore the reported jitter value here is not necessarily the best timing resolution of the tested device. However, it provides some insight into the overall system set up and the temporal characteristics of InGaAs/InP SPADs.

IV. Conclusion

We report an InGaAs/InP SPAD pair operated with 70 MHz sinusoidal gating at wavelength of 1310 nm. At a laser repetition rate of 1 MHz, photon detection efficiency of 43% has been achieved with dark count rate of 58 kHz at 240 K. At photon detection efficiency of ~10%, DCR is 9.6 kHz; the equivalent dark count probability is 2.8×10^{-5}. The afterpulsing probability is compared with gated PQAR and conventional sinusoidal gating. At higher repetition rate and the same PDE, the afterpulse probability has been reduced compared with a sinusoidal gated single SPAD. The lower afterpulsing is explained in terms of the integrated excess bias over time, Δ, and some cancellation of dark counts in the SPAD pair. Parameters that affect afterpulsing in sinusoidal gating have also been discussed. The parameter Δ provides insight into the nature of sinusoidal gating and its effects on the performance of SPADs.

References

[1] Z. L. Yuan, A. W. Sharpe, J. F. Dynes, A. R. Dixon, and A. J. Shields, "Multi-gigahertz operation of photon counting InGaAs avalanche photodiodes," *Appl. Phys. Lett.*, vol. 96, no. 7, pp. 071101-1–071103, 2010.

[2] J. Zhang, R. Thew, C. Barreiro, and H. Zbinden, "Practical fast gate rate InGaAs/InP single-photon avalanche photodiodes," *Appl. Phys. Lett.*, vol. 95, pp. 091101–091103, Aug. 2009.

[3] Y. Nambu, S. Takahashi, K. Yoshino, A. Tanaka, M. Fujiwara, M. Sasaki, A. Tajima, S. Yorozu, and A. Tomita, "Efficient and low-noise single-photon avalanche photodiode for 1.244-GHz clocked quantum key distribution," *Opt. Exp.*, vol. 19, pp. 20531–20541, Aug. 2011.

[4] N. Namekata, S. Adachi, and S. Inoue, "1.5 GHz single-photon detection at telecommunication wavelengths using sinusoidally gated InGaAsInP avalanche photodiode," *Opt. Exp.*, vol. 17, no. 8, pp. 6275–6282, 2009.

[5] Z. Lu, X. Zheng, W. Sun, J. C. Campbell, X. Jiang, and M. A. Itzler, "Characterization of sinusoidal gating of InGaAs/InP single photon avalanche diodes," *Proc. SPIE*, vol. 8375, no. 1, pp. 26–35, Apr. 2012.

[6] D. S. Bethune and W. P. Risk, "An autocompensating fiber-optic quantum cryptography system based on polarization splitting of light," *IEEE J. Quantum Electron.*, vol. 36, no. 3, pp. 340–347, Mar. 2000.

[7] A. Tosi, A. D. Mora, A. D. Frera, A. B. Shehata, A. Pifferi, and D. Contini, "Fast-gated SPAD for ultrawide dynamic range optical investigations," in *Proc. IEEE 23rd Annu. Photon. Soc. Meeting Conf.*, Nov. 2010, pp. 185–186.

[8] A. Restelli and J. C. Bienfang, "Avalanche discrimination and high-speed counting in periodically gated single-photon avalanche diodes," *Proc. SPIE*, vol. 8375, pp. 83750-1–83750-8, Apr. 2012.

[9] Q.-L. Wu, Y. Liu, Z.-F. Han, W. Chen, Y.-M. Dai, G. Wei, and G.-C. Guo, "Gated-mode integrated single photon detector for telecom wavelengths," *Adv. Photon. Count. Technol.*, vol. 6771, pp. 67711-1–67711-7, Apr. 2007.

[10] A. Tomita and K. Nakamura, "Balanced, gated-mode photon detector for quantum-bit discrimination at 1550 nm," *Opt. Lett.*, vol. 27, no. 20, pp. 1827–1829, 2002.

[11] N. Namekata, S. Sasamori, and S. Inoue, "800 MHz single-photon detection at 1550-nm using an InGaAsInP avalanche photodiode operated with a sine wave gating," *Opt. Exp.*, vol. 14, no. 21, pp. 10043–10049, 2006.

[12] J. Zhang, P. Eraerds, N. Walenta, C. Barreiro, R. Thew, and H. Zbinden, "2.23 GHz gating InGaAs/InP single-photon avalanche diode for quantum key distribution," *Proc. SPIE*, vol. 7681, pp. 1–8, Apr. 2010.

[13] M. Liu, C. Hu, J. C. Campbell, P. Zhong, and M. M. Tashima, "Reduce afterpulsing of single photon avalanche diodes using passive quenching with active reset," *IEEE J. Quantum Electron.*, vol. 44, no. 5, pp. 430–434, May 2008.

[14] C. Hu, X. Zheng, J. C. Campbell, B. M. Onat, X. Jiang, and M. A. Itzler, "Characterization of an InGaAs/InP-based single-photon avalanche diode with gated-passive quenching with active reset circuit," *J. Modern Opt.*, vol. 58, pp. 201–209, Feb. 2011.

[15] A. W. Lightstone and R. J. McIntyre, "Photon counting silicon avalanche photodiodes for photon correlation spectroscopy," *Photon Correl. Technol. Appl.*, vol. 32, no. 21, pp. 183–189, 1988.

[16] S. Cova, M. Ghioni, A. Lacaita, C. Samori, and F. Zappa, "Avalanche photodiodes and quenching circuits for single-photon detection," *Appl. Opt.*, vol. 35, no. 12, pp. 1956–1976, 1996.

[17] G. P. Agrawal, *Fiber-Optic Communications Systems*. New York: Wiley, 2002.

[18] G. Blyth. (2012). *Differential Signaling* [Online]. Available: http://en.wikipedia.org/wiki/Differential_signaling

[19] Z. L. Yuan, B. E. Kardynal, A. W. Sharpe, and A. J. Shields, "High speed single photon detection in the near infrared," *Appl. Phys. Lett.*, vol. 91, no. 4, pp. 041114-1–041114-3, 2007.

[20] Z. Lu, Y. Kang, C. Hu, Q. Zhou, H.-D. Liu, and J. C. Campbell, "Geiger-mode operation of Ge-on-Si avalanche photodiodes," *IEEE J. Quantum Electron.*, vol. 47, no. 5, pp. 731–735, May 2011.

[21] M. A. Itzler, M. Entwistle, and X. Jiang, "High-rate photon counting with geiger-mode APDs," in *Proc. IEEE Photon. Annu. Meeting*, Oct. 2011, pp. 348–349.

[22] M. A. Itzler, X. Jiang, M. Entwistle, K. Slomkowski, A. Tosi, F. Acerbi, F. Zappa, and S. Cova, "Advances in InGaAsP-based avalanche diode single photon detectors," *J. Modern Opt.*, vol. 58, nos. 3–4, pp. 174–200, 2011.

Joe C. Campbell (S'73–M'74–SM'88–F'90) received the B.S. degree from the University of Texas at Austin, Austin, in 1969, and the M.S. and Ph.D. degrees from the University of Illinois at Urbana-Champaign, Champaign, in 1971 and 1973, respectively, all in physics.

He was with Texas Instruments, Dallas, where he was engaged in research on integrated optics, from 1974 to 1976. In 1976, he joined the AT&T Bell Laboratories, Holmdel, NJ, as a Staff Member, where he was involved in research on a variety of optoelectronic devices, including semiconductor lasers, optical modulators, waveguide switches, photonic integrated circuits, and photodetectors, with emphasis on high-speed avalanche photodiodes for high-bit-rate lightwave systems. In 1989, he joined the University of Texas at Austin as a Professor of electrical and computer engineering and as the Cockrell Family Regents Chair in Engineering. In 2006, he became a Faculty Member with the University of Virginia, Charlottesville, and then the Lucian Carr and the III Chair of Electrical Engineering and Applied Science. He has co-authored 320 papers for refereed technical journals, more than 200 conference presentations, and 6 book chapters. His research focused on the optoelectronic components that are used to generate, modulate, and detect the optical signals. His current research interests include single-photon-counting avalanche photodiodes, Si-based optoelectronics, high-speed low-noise avalanche photodiodes, ultraviolet photodetectors, and quantum-dot IR imaging.

Dr. Campbell is a member of the National Academy of Engineering and a fellow of the Optical Society of America and the American Physical Society.

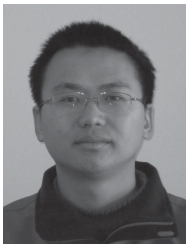

Wenlu Sun was born in Puyang, China, in 1989. He received the B.S. degree in physics from the University of Science and Technology of China, Hefei, China, in 2009. He is currently pursuing the Ph.D. degree with the Department of Electrical Engineering, University of Virginia, Charlottesville.

His current research interests include low-noise avalanche photodiodes and single-photon counting.

Zhiwen Lu received the B.S. degree in physics from the University of Science and Technology of China, Hefei, China, in 2007, and the M.E. degree in electrical engineering from the University of Virginia, Charlottesville, in 2009, where she is currently pursuing the Ph.D. degree in electrical engineering.

Her current research interests include infrared single-photon avalanche diodes, low-noise avalanche photodiodes, and quantum-dot infrared photodiodes.

Mark A. Itzler received the B.S. degree from Brown University, Providence, RI, and the Ph.D. degree from the University of Pennsylvania, Philadelphia, in 1986 and 1992, respectively, both in physics.

He was a Post-Doctoral Researcher with Harvard University, Cambridge, MA, from 1992 to 1995. He joined Epitaxx Optoelectronics, Inc., West Trenton, NJ, in 1996, where he was promoted to the Director of R&D in 1999. Following the acquisition of Epitaxx by JDS Uniphase in 1999, he became the Chief Technical Officer (CTO) and the Vice President of Device Engineering, Epitaxx Division, JDSU, in 2000. In 2003, he joined Princeton Lightwave Inc. (PLI), Cranbury, NJ, as the CTO, where he led the development of high-performance photodetector technology and provided oversight for the company's other device technology programs, and became the CEO in 2012. He has authored or co-authored over 75 technical papers and conference presentations, and holds 14 patents. His current research interests include semiconductor photodetectors, particularly in single-photon counting and avalanche photodiodes.

Dr. Itzler was the Chair of the IEEE Photonics Society (formerly LEOS) Technical Committee on Photodetectors and Imaging, and he is the Chair of the Advanced Photon Counting Techniques Conference held as part of the SPIE Defense, Security, and Sensing Symposium. He is an Associate Editor of the IEEE PHOTONICS TECHNOLOGY LETTERS.

Xudong Jiang received the B.S., M.S., and Ph.D. degrees in physics from Beijing University, Beijing, China, in 1989, 1992, and 1995, respectively.

He was a Post-Doctoral Researcher with Harvard University, Cambridge, MA, from 1995 to 1996, and Princeton University, Princeton, NJ, from 1996 to 1997, and involved in research on electrical and optical properties of superlattices and thin-film transistors. He joined the University of Florida, Gainesville, as the Co-Principal Investigator on a project funded by the U.S. Army Research Office and focused on MWIR and LWIR quantum well infrared photodetector design, processing, and characterization from 1997 to 2000. He joined Multiplex, Inc., South Plainfield, NJ, in 2000, where he was engaged in the development and manufacturing of 980-nm pump laser and electroabsorption-modulated laser devices and modules, and was promoted as a Distinguished Member of the Technical Staff in 2002 and the Manager of Laser Engineering and Operation in 2003. In 2006, he joined Princeton Lightwave Inc., Cranbury, NJ, where he is currently a Senior Staff Engineer and leads programs focused on the design and characterization of high-performance photodetectors and detector-based products. He has authored or co-authored more than 40 technical publications.